Progress with Applications of Three-Ion ICRF Scenarios for Fusion Research: a Review

Ye.O. Kazakov[1,a)], J. Ongena[1], M. Nocente[2,3], V. Bobkov[4], J. Garcia[5], V.G. Kiptily[6], M. Schneider[7], S. Wukitch[8], J.C. Wright[8], M. Dreval[9,10], K.K. Kirov[6], S. Mazzi[5], R. Ochoukov[4], S.E. Sharapov[6], Ž. Štancar[6], H. Weisen[11], Y. Baranov[6], M. Baruzzo[12], A. Bierwage[13,14], R. Bilato[4], A. Chomiczewska[15], R. Coelho[16], T. Craciunescu[17], K. Crombé[1], E. Delabie[18], E. de la Luna[19], R. Dumont[5], P. Dumortier[1], F. Durodié[1], J. Eriksson[20], M. Fitzgerald[6], J. Galdon-Quiroga[21], D. Gallart[22], M. Garcia-Munoz[21], L. Giacomelli[2], C. Giroud[6], J. Gonzalez-Martin[21], A. Hakola[23], R. Henriques[6,16], P. Jacquet[6], I. Jepu[6,17], T. Johnson[24], A. Kappatou[4], D. Keeling[6], D. King[6], C. Klepper[18], Ph. Lauber[4], M. Lennholm[6], E. Lerche[1], B. Lomanowski[18], C. Lowry[6], M.J. Mantsinen[22,25], M. Maslov[6], S. Menmuir[6], I. Monakhov[6], F. Nabais[16], M.F.F. Nave[16], C. Noble[6], E. Panontin[3], S.D. Pinches[7], A.R. Polevoi[7], D. Rigamonti[3], A. Sahlberg[19], M. Salewski[26], P.A. Schneider[4], H. Sheikh[6], K. Shinohara[27], P. Siren[6], S. Sumida[14], A. Thorman[6], R.A. Tinguely[8], D. Valcarcel[6], D. Van Eester[1], M. Van Schoor[1], J. Varje[11], M. Weiland[4], N. Wendler[15], JET Contributors*, the ASDEX Upgrade Team** and the EUROfusion MST1 Team***

[1] Laboratory for Plasma Physics, LPP-ERM/KMS, Royal Military Academy, Brussels, Belgium;
[2] Dipartimento di Fisica, Università di Milano-Bicocca, Milan, Italy;
[3] Institute for Plasma Science and Technology, National Research Council, Milan, Italy;
[4] Max-Planck-Institut für Plasmaphysik, Garching, Germany;
[5] CEA, IRFM, Saint-Paul-Lez-Durance, France;
[6] United Kingdom Atomic Energy Authority (UKAEA), Culham Centre for Fusion Energy (CCFE), Culham Science Centre, Abingdon, UK;
[7] ITER Organization, Route de Vinon-sur-Verdon, 13067 St. Paul-lez-Durance, France;
[8] Plasma Science and Fusion Center, MIT, Cambridge MA, USA;
[9] V.N. Karazin Kharkiv National University, Kharkiv, Ukraine;
[10] NSC 'Kharkiv Institute of Physics and Technology', Kharkiv, Ukraine;
[11] Tokamak Energy Ltd, Milton Park, United Kingdom;
[12] ENEA for EUROfusion, Frascati (Roma), Italy;
[13] QST Rokkasho Fusion Institute, Rokkasho, Japan; [14] QST Naka Fusion Institute, Ibaraki, Japan;
[15] Institute of Plasma Physics and Laser Microfusion (IPPLM), Warsaw, Poland;
[16] Instituto de Plasmas e Fusão Nuclear, IST, Lisbon, Portugal;
[17] National Institute for Laser, Plasma and Radiation Physics (NILPRP), Bucharest, Romania;
[18] Oak Ridge National Laboratory, Oak Ridge, USA;
[19] Laboratorio Nacional de Fusión, CIEMAT, Madrid, Spain; [20] Uppsala University, Uppsala, Sweden;
[21] University of Seville, Seville, Spain; [22] Barcelona Supercomputing Center (BSC), Barcelona, Spain;
[23] VTT Technical Research Centre of Finland, Espoo, Finland;
[24] KTH Royal Institute of Technology, Stockholm, Sweden; [25] ICREA, Barcelona, Spain;
[26] Dept. of Physics, Technical University of Denmark, Kgs. Lyngby, Denmark;
[27] The University of Tokyo, Kashiwa, Japan;

** See the author list of J. Mailloux et al., Nucl. Fusion 62, 042026 (2022)*
*** See the author list of H. Meyer et al., Nucl. Fusion 59, 112014 (2019)*
**** See the author list of B. Labit et al., Nucl. Fusion 59, 086020 (2019)*

[a)] Corresponding author: yevgen.kazakov@rma.ac.be

Abstract. The success of magnetic confinement fusion as an energy source relies crucially on reaching the necessary high temperatures for the fuel D and T ions. In a fusion reactor, plasma heating with waves in the ion cyclotron range of frequencies (ICRF) is the only system capable of providing a large fraction of bulk ion heating. Furthermore, in view of a better understanding of the non-linear physics of alpha heating in ITER and future reactors, generating MeV-range ions and studying the impact of fast ions on plasma stability and confinement becomes progressively more important. This paper summarizes recent theoretical progress and experimental demonstrations of the so-called three-ion ICRF scenario on the tokamaks Alcator C-Mod, ASDEX Upgrade and JET. In particular, the paper highlights several key results relevant for ITER and future fusion reactors.

INTRODUCTION

Auxiliary plasma heating is essential for future fusion reactors to reach high ion temperatures necessary for the D-T fusion. Plasma heating with waves in the ion cyclotron range of frequencies (ICRF) is a flexible technique for which several efficient heating scenarios have been developed [1–4]. The so-called minority heating scenarios [5] are widely used in toroidal magnetic fusion research, as they are characterized by strong damping of the RF waves propagating in the plasma. These scenarios rely on fundamental ion cyclotron absorption ($\omega = \omega_{ci} + k_{\|}v_{\|}$) of electromagnetic waves by a small number of resonant ions with a different cyclotron frequency than that of the main plasma ions. In turn, these RF-heated minority ions transfer their energy via Coulomb collisions to the other plasma particles, bulk ions and electrons. The fraction of bulk ion and electron heating depends on the ratio of the fast-ion energy to the critical energy E_{crit} defined as $E_{\rm crit} = 14.8 A_{\rm fast} T_e (\sum_i X_i Z_i^2/A_i)^{2/3}$ [6]. Here, A_{fast} is the atomic mass of the energetic ions, T_e is the electron temperature, and $X_i = n_i/n_e$, Z_i, and A_i are the concentration, the charge state, and the atomic mass of the thermal ion species, respectively. As a result, for typical plasma parameters in magnetic fusion devices, fast ions with MeV-range energies heat primarily plasma electrons. Nevertheless, it is possible to achieve also dominant heating of the bulk ions by selecting ions with a higher atomic mass as RF absorbing ions and by tailoring the fast-ion energies in the range of E_{crit} or below.

Recent theoretical and experimental developments have demonstrated the existence of a new class of efficient RF heating schemes, hereafter referred to as 'three-ion ICRF scenarios' [7–10]. These novel scenarios are relevant for heating various plasma mixtures composed of H and He isotopes, e.g. D-T, H-D, H-^{4}He, D-^{3}He plasmas, and in addition can make use of intrinsic and extrinsic impurities such as ^{9}Be, Ne, Ar, etc. to optimize the application of ICRF power in fusion devices.

In general, these novel scenarios require the plasma composition to be extended beyond two thermal ion species by providing an additional ('third') ion population. A proper choice for the plasma composition is required such that the third ion population satisfies the resonant condition $\omega = \omega_{ci} + k_{\|}v_{\|}$ in the vicinity of one of the ion-ion hybrid (IIH) layers in those multi-ion species plasmas, where the left-hand polarized RF electric field component (rotating in the direction of the plasma ions) is strongly enhanced [11, 12].

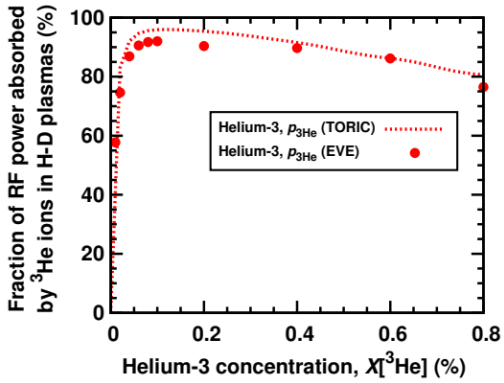

FIGURE 1. Three-ion ICRF scenarios and their high potential for generating fast ions in fusion plasmas were identified in Ref. [7]. The figure shows one of the main results predicted by theory: efficient absorption of RF power by a very small number of ^{3}He ions (e.g., at $n(^3He)/n_e \approx 0.1$-0.2%) in mixed H-D ≈ 70%-30% plasmas. Figure reproduced from Ref. [7].

Throughout the paper, we use the following notation for three-ion ICRF scenarios Y_2-(Y_3)-Y_1. Here, indices '1' and '2' are used for the non-resonant ion species Y_1 and Y_2 (ordered according to their Z/A value, i.e. $\omega_{c2} < \omega_{c1}$), and index '3' is reserved for the resonant ions Y_3 (indicated between the round brackets). In fact, there are two equivalent possibilities for the choice of the resonant absorbers. The original theoretical formulation of these ICRF scenarios in Ref. [7] proposed a population of ions with a charge-to-mass ratio 'sandwiched' between that of the two non-resonant ions, $(Z/A)_2 < (Z/A)_3 < (Z/A)_1$. In this case, the ion cyclotron absorption by resonant ions at extremely low concentrations (as low as a few per mille, %) is maximized in multi-ion plasmas with $X_1 \gtrsim X_1^*$ and $X_2 \lesssim X_2^*$, where

$$X_1^* = \frac{1}{Z_1}\frac{(Z/A)_1 - (Z/A)_3}{(Z/A)_1 - (Z/A)_2}, X_2^* = \frac{1}{Z_2}\frac{(Z/A)_3 - (Z/A)_2}{(Z/A)_1 - (Z/A)_2}\,. \quad (1)$$

This maximizes the absorbed RF power per resonant ion and thus strongly enhances the efficiency of fast-ion generation with ICRF. As an example, Figure 1 shows the computed fraction of RF power absorbed by ^{3}He ions in mixed H-D = 70%-30% plasmas at JET, illustrating that nearly all RF power can be channelled to ^{3}He ions at concentrations as low as $n(^3\text{He})/n_e \approx 0.1\text{-}0.2\%$.

Fast ions with the same charge-to-mass ratio as one of the main plasma ions can also be used as resonant absorbers [9]. To make the heating scenario work, the third ion population should have sufficiently large parallel velocities such that they can resonate at the IIH layer because of their large Doppler shift. Fast ions injected by neutral beam injection (NBI) are a natural choice for the realization of the Doppler-shifted version of the three-ion ICRF scenario. This technique allows to explore new synergies between ICRF and NBI heating systems, and to accelerate fast ions from their starting energies on the order of 100 keV (typical for the NBI systems in present-day tokamaks) to MeV-range energies. Furthermore, as discussed below, the application of this synergetic ICRF-NBI scenario at JET leads to a very efficient generation of passing fast ions, and thus the resulting fast-ion distribution mimics closely the distributions generated by negative-NBI systems in the future tokamaks JT-60SA and ITER. For the plasma composition required to realize this ICRF scenario, we refer to Eqs. (6) and (7) in Ref. [10].

EU-US COLLABORATION: PROOF-OF-PRINCIPLE EXPERIMENTS ON ALCATOR C-MOD, JET AND ASDEX UPGRADE TOKAMAKS

Theoretical and modeling results predicting a high efficiency of these novel ICRF scenarios were presented at the 21st RF Topical Conference in April 2015 (Lake Arrowhead, USA) [13]. Following the discussions at this conference, a collaborative effort between EU and US researchers was established, aiming at the experimental verification of the potential of these novel scenarios on existing tokamaks. In 2015-2016, a series of proof-of-principle ICRF studies was conducted on Alcator C-Mod (MIT-PSFC, USA) and JET (Culham, UK). First results on both devices were encouraging and confirmed theoretical predictions. Indeed, as shown in Fig. 2, both experiments successfully demonstrated the high efficiency of the three-ion D-(^{3}He)-H ICRF scenario for heating mixed H-D plasmas with a small amount of ^{3}He ions. Whereas the optimal ^{3}He concentration for this scenario in Alcator C-Mod was approximately $n(^3\text{He})/n_e \approx 0.5\%$, even lower ^{3}He concentrations ~0.2% were successfully applied in JET experiments.

Both tokamak experiments also confirmed the high efficiency of these novel ICRF scenarios for generating energetic ions in the plasma. This was evidenced, e.g., by the sawtooth stabilization and the observation of fast-ion-driven Alfvén eigenmodes (see the right panel of Fig. 2(a) for Alcator C-Mod results). The efficiency of fast ^{3}He generation in JET plasmas was further enhanced by choosing the asymmetric co-current ICRF antenna phasing and exploiting the RF-induced pinch effect [14, 15]. The strong core localization of fast ^{3}He ions in JET plasmas was independently confirmed by gamma-ray measurements. The right panel of Figure 2(b) shows the poloidal cross-section of the plasma in JET pulse #90753 (3.2T/2.0MA, $f \approx 33$ MHz) together with the reconstructed high-energy gamma-ray emission. Note that most of the energetic ^{3}He ions are strongly localized in the plasma core and have passing (stagnation) orbits [16]. A summary of main findings of the proof-of-principle Alcator C-Mod and JET experiments with the three-ion D-(^{3}He)-H ICRF scenario was published in the October 2017 issue of the journal Nature Physics [8].

In July 2016, the Doppler-shifted three-ion ICRF scenario with fast D-NBI ions ($E_{NBI} \approx 100$ keV) as resonant absorbers in mixed H-D plasmas was first demonstrated on JET. An overview of the results obtained with this scenario was presented at the 22nd RF Topical Conference in June 2017 (Aix-en-Provence, France) [9], later detailed in [17]. The fast-ion observations were successfully reproduced by TRANSP-TORIC and PION modeling [17, 18]. As shown by the tomographic reconstruction of the neutron emission, MeV-range D ions generated with this D-(D_{NBI})-H scenario are also strongly core localized (see also [20]) and have the same orbit topology as resonant ^{3}He ions in the D-(^{3}He)-H ICRF experiments. The important consequences of this rather special topology for the resonant fast ions will be discussed in the next sections of this paper.

For the experimental verification of these novel and highly efficient ICRF scenarios on EU and US tokamaks, the 2018 APS-EPS Landau-Spitzer Award was granted to the leading four authors of Ref. [8].

In July 2017, the three-ion D-(^{3}He)-H ICRF scenario was demonstrated also on the tokamak ASDEX Upgrade (Garching, Germany) [10, 21]. Guided by the ITER needs, significant progress with the development of these ICRF scenarios has been achieved on JET and AUG, as detailed in the Physics of Plasmas review paper [10]. Further progress has been achieved since then, including the application of these ICRF scenarios in non-active and D-T plasmas, relevant for ITER. In what follows, the key observations from these new experiments are summarized.

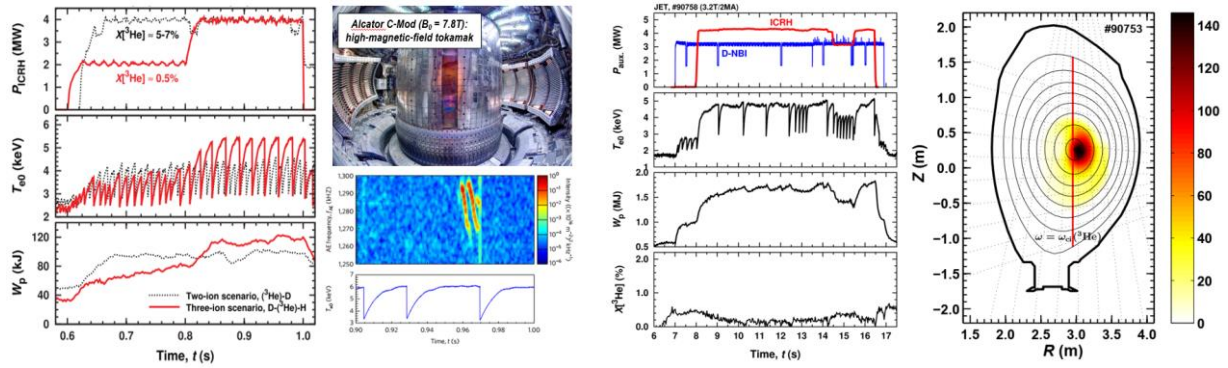

FIGURE 2. The high efficiency of three-ion ICRF scenarios for plasma heating and generation of energetic ions in the plasma was successfully demonstrated in proof-of-principle experiments on (a) Alcator C-Mod and (b) JET tokamaks. The right panel of Fig. 2(a) shows the sawtooth stabilization and the observation of fast-ion-driven Alfvén eigenmodes in Alcator C-Mod experiments. The right panel of Fig. 2(b) shows the JET plasma poloidal cross-section together with the reconstructed high-energy gamma-ray emission, visualizing the population of the confined energetic ^{3}He ions with $E(^3\text{He}) > 1$-2 MeV. Note that most of energetic ^{3}He ions are strongly localized in the plasma core and have passing (stagnation) orbits [16]. Figures reproduced from Ref. [8].

FAST IONS AS A TOOL FOR PLASMA CONTROL AND ENHANCED PERFORMANCE AT JET

Megaelectron volt (MeV) alpha particles will be the main source of plasma heating future in magnetic confinement fusion reactors. Yet instead of heating fuel ions, most of the energy of the alpha particles is transferred to the electrons. The temperature of the fuel D and T ions in these plasmas will be largely determined by the combined effect of the transfer of power from electrons to bulk ions, and the ion-temperature-gradient (ITG) instability. A beneficial impact of alpha particles on the ITG instability in high-beta ITER plasmas was recently predicted [22].

Furthermore, the presence of alpha particles in fusion plasmas is expected to generate a range of fast-ion phenomena, including the stabilization of sawtooth oscillations, possible destabilization of different types of fast-ion-driven Alfvén eigenmodes (AEs), the modification of the plasma equilibrium, etc. In most of present-day fusion experiments, the fraction of MeV-range fast ions in the plasma core is fairly low and therefore fast-ion effects – to a large extent – can be studied individually [23]. However, a non-linear coupling between different fast-ion effects is expected in future burning plasmas, including the impact of fast ions on the ITG instability. Altogether this makes the extrapolation of alpha heating in future plasmas not straightforward, and underlines the need for experimental studies, accompanied by modeling of plasmas with a large population of MeV-range fast ions in present-day devices.

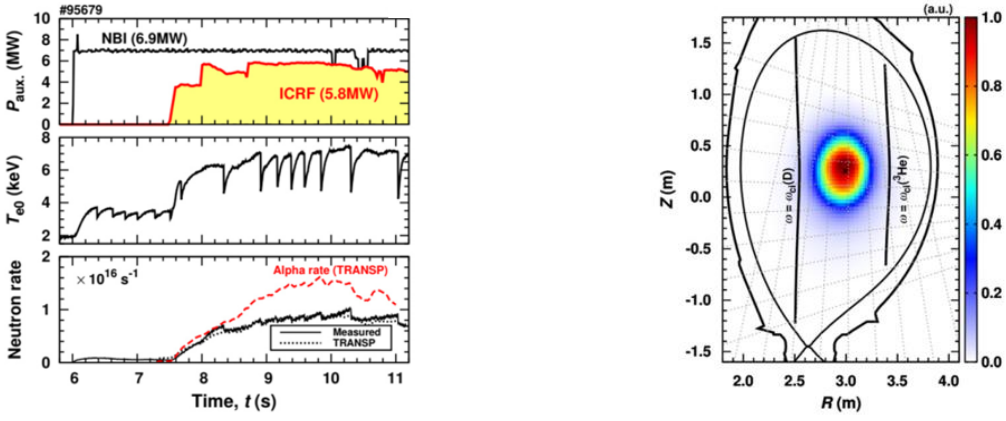

FIGURE 3. JET studies with the three-ion D-(D_{NBI})-^{3}He scenario in D-^{3}He plasmas revealed a range of new synergistic fast-ion phenomena, relevant for ITER and future burning plasmas. (a) Overview of JET pulse #95679 (3.7T/2.5MA, $n_{e0} \approx 6\times10^{19}$ m^{-3}, $n(^3\text{He})/n_e \approx$ 20-25%, $P_{NBI} \approx 6.9$ MW, $P_{ICRF} \approx 5.8$ MW, $f \approx 33.0$ MHz, dipole phasing). Note the strong increase in the neutron and alpha-particle generation rates during the combined ICRF + NBI heating phase. (b) The measured spatial profile of the D-D neutron emission, clearly illustrating the generation of high-energy D ions in the plasma core with this novel ICRF scheme. The figure also shows the location of the ion cyclotron resonances for thermal D and ^{3}He ions (both off-axis). Figure reproduced from Ref. [26].

For a deeper understanding of the dynamics of such plasmas, a series of dedicated experiments in D-^{3}He plasmas was conducted at JET with the three-ion D-(D_{NBI})-^{3}He ICRF scenario [10, 24]. This scenario was chosen as it allows to accelerate the neutral beam injection (NBI) deuterons with starting energies of ~100 keV to higher energies using ICRF waves. The developed experimental scenario provided unique conditions on JET for probing several aspects of future burning plasmas (e.g. studying the impact of MeV-range fast ions on global plasma confinement), without having to introduce tritium. Figure 3 shows an overview of JET pulse #95679 (3.7T/2.0MA, $n(^3\text{He})/n_e \approx$ 20-25%, $f \approx$ 33 MHz, dipole phasing), in which ~6 MW of ICRF was applied in combination with ~7 MW of NBI. Because of the efficient generation of MeV-range deuterium ions with this ICRF scheme, the D-D neutron rate increased from ~0.6×10^{15} s^{-1} in the NBI-only phase to ~1.0×10^{16} s^{-1} in the combined ICRF + NBI phase of the pulse. These JET plasmas also included a significant population of core-localized alpha particles originating from D-^{3}He fusion reactions ($E_\alpha \approx$ 3.6 MeV) [25]. As follows from Fig. 3(a), the production rate of alpha particles in these plasmas, $R_\alpha \approx$ 1-2×10^{16} s^{-1} exceeded the D-D neutron rate [26].

Contrary to expectations, an efficient increase in T_i of the bulk ions in the presence of dominant fast-ion electron heating and strong fast-ion driven Alfvénic instabilities was observed in these experiments, resulting in $T_i \approx T_e$. Detailed transport analysis revealed that the ITG turbulence in these JET plasmas was nearly suppressed, in the presence of a large number of MeV-range fast ions in the plasma core and fully developed Alfvénic activities [27, 28]. This nonlinear mechanism holds promise for a more economical operation in ITER and future fusion reactors with dominant alpha particle heating.

Figures 4(a) and (b) illustrate the typical distribution of ICRF-accelerated D ions (as computed by the TRANSP-TORIC code, see [29]) and the characteristic orbit of resonant D ions (white line), respectively. The figure demonstrates a unique feature of this ICRF scenario at JET: the capability to generate a large amount of high-energy passing (stagnation) ions ($E_D \sim$ 1 MeV, $\lambda = v_\parallel/v \approx$ 0.3-0.5) [24]. We note that the applied three-ion ICRF scheme generates a fast-ion population with similar characteristics as high-energy N-NBI systems at JT-60U, JT-60SA and ITER, thereby allowing to study different aspects of the interaction of super-Alfvénic passing fast ions also at JET. A detailed discussion on the efficiency of this three-ion ICRF scheme for generating passing fast ions and fast-ion current drive can be found in Section III-B in Ref. [10]. In short, the energy-dependence of the pitch parameter of the resonant ions, $\lambda = v_\parallel/v$ is given by

$$\lambda(E) = \sqrt{\lambda_0^2 \frac{E_0}{E} + \lambda_\infty^2 \left(1 - \frac{E_0}{E}\right)}, \tag{2}$$

where λ_0 and E_0 are the initial pitch and energy of resonant ions ($\lambda_0 \approx$ 0.62 and $E_0 \approx$ 100 keV in case of tangential NBI injectors at JET); $\lambda_\infty = (1 - \Lambda_\infty)^{1/2}$, and $\Lambda_\infty = \omega_{cD}(0)/\omega \approx$ 0.85-0.89. Thus, at high energies the pitch parameter of the ICRF-accelerated deuterons reaches $\lambda_\infty \approx$ 0.34-0.38, consistent with modeling results.

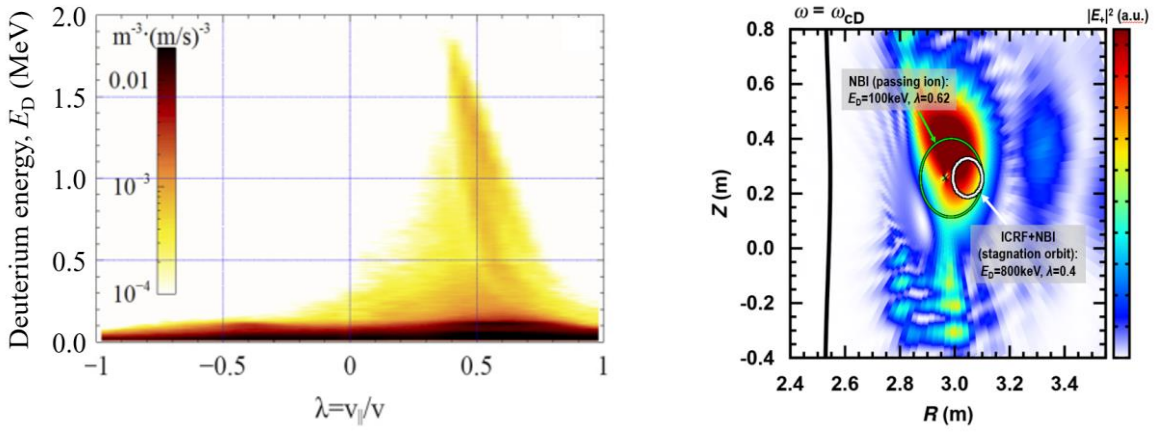

(a) (b)

FIGURE 4. Three-ion ICRF scenarios are efficient in generating a large amount of passing fast ions ($v_\parallel > 0$) at JET. (a) A typical distribution function of the energetic D ions generated with the D-(D_{NBI})-^{3}He scenario, as computed by the TRANSP-TORIC code. (b) A characteristic orbit of resonant D ions (E_D = 0.8 MeV, λ = 0.4, white curve), together with the computed distribution of $|E_+|^2$, as evaluated by TORIC. The figure also shows the computed orbit of the passing NBI fast ions with E_D = 0.1 MeV and λ = 0.62 (green curve). Figure 4(a) is reproduced from Ref. [32].

A broad range of AEs was destabilized by fast ions in JET D-^{3}He plasmas heated with the three-ion ICRF scenario [30-34], see Fig. 5(a). The observed modes include the toroidicity-induced AEs (TAEs), ellipticity-induced AEs (EAEs), as well as reversed-shear AEs (RSAEs), originating from the presence of a local minimum in the safety factor q_{min}. Two different types of centrally localized RSAEs were regularly observed during the long-period sawtooth phases in this series of JET experiments [32]. In addition to the low-frequency RSAEs with frequencies below the TAE frequency ($f \approx$ 80-180 kHz), also high-frequency RSAEs with frequencies above the TAE frequency ($f \approx$ 330-450 kHz) were excited. Such high-frequency RSAEs were previously reported in reversed-shear plasmas in JT-60U heated with the negative-ion NBI system [35]. This shows again a similarity between fast-ion populations generated by high-energy N-NBI systems and the three-ion ICRF scenario at JET.

As follows from Fig. 5(b), the destabilization of this mode in JET plasmas requires the presence of MeV-range passing fast D ions with $\lambda \approx$ 0.3-0.5. Traditionally used ICRF schemes usually generate fast ions with $\lambda \approx 0$. In contrast, the fast-ion population generated by the three-ion ICRF scheme includes a large number of passing fast ions with large values of λ, capable to interact resonantly with these modes. This explains why the high-frequency RSAEs were not studied at JET before. Simultaneously, the RF-accelerated D ions are also efficient to drive a local fast-ion current, resulting in plasmas with an inverted q-profile. This was independently confirmed by MSE measurements ($q_{min} \approx$ 0.80-0.85 at $R_{min} \approx$ 3.2 m) [32], as shown in Fig. 5(c).

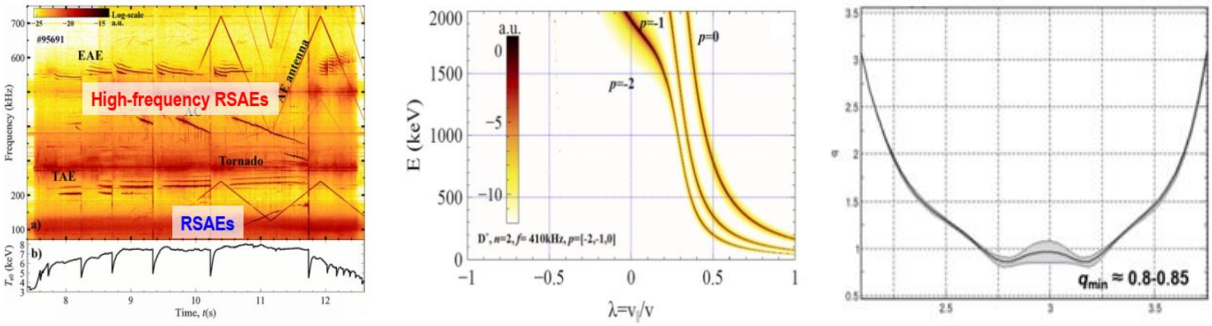

(a) (b) (c)

FIGURE 5. The three-ion D-(D_{NBI})-^{3}He ICRF scenario at JET is efficient for generating passing fast ions and for local fast-ion current drive. This results in plasmas with an inverted q-profile and the destabilization of reversed-shear AEs, including high-frequency RSAEs, observed previously in N-NBI experiments on JT-60U. (a) High-frequency RSAEs in JET pulse #95691. (b) The computed resonant map for the n = 2 high-frequency RSAE interacting with D ions. (c) The q-profile in JET pulse #95691, as inferred by the MSE diagnostic. Figures reproduced from Ref. [32].

As discussed in [24], the sawtooth period in these fast-ion experiments varied between 200-300 ms and a few seconds, in the presence of EAEs and RSAEs. The simultaneous observation of EAEs with the toroidal mode number n = -1 and the axisymmetric mode with n = 0 in the frequency range of EAEs was unexpected. Indeed, as follows from the analysis in [33, 34], the destabilization of the n = -1 EAE requires the presence of high-energy ions with $\lambda < 0$. Such fast ions, moving in the counter-current direction, are virtually absent in the fast-ion population generated by the three-ion ICRF scenario (see Fig. 4(a)). In contrast, the pitch-angle distribution of D-^{3}He fusion-born alpha particles naturally covers the full range of pitch parameters from λ = -1 to λ = +1, thus providing a source of particles circulating in the counter-current direction.

The presence of regular sawtooth crashes in these plasmas leads to a modulation of the D-^{3}He fusion power. As a result, when the sawtooth period is shorter than the characteristic slowing-down time of alphas, a bump-on-tail distribution for the fusion-born alphas can be developed, necessary for the destabilization of the n = 0 mode [33, 34]. The energy-selective confinement of fusion-born alpha particles during sawtooth crashes in these JET plasmas was recently studied in Ref. [36].

The JET results and new phenomena discussed above illustrate the complex interplay between fast ions, monster sawtooth crashes, AEs and plasma confinement. These surprising observations highlight the need for further studies of the synergies between different fast ion phenomena in future burning plasmas (see also a discussion in [23]).

PHYSICS STUDIES IN NON-ACTIVE H-^{4}HE PLASMAS ON AUG AND JET

Reaching good-quality H-mode and developing ELM control techniques are among the main priorities for ITER during its non-active operations [37]. Recent encouraging experimental results at JET-ILW demonstrated a significant reduction in the H-mode power threshold for NBI-heated plasmas when a small amount of ^{4}He ions, $n(^4\text{He})/n_e \approx 10\%$, was added to hydrogen plasmas [38]. This finding motivated the ITER team to consider the use of H-^{4}He plasmas to widen the H-mode operational space in predominantly hydrogen plasmas. Equally important, this mix also allows the application of the three-ion ICRF scheme with off-axis heating of ^{3}He minority ions at concentrations $n(^3\text{He})/n_e < 1\%$, as proposed in [39], allowing to deposit additionally up to 20 MW of heating power in H + 10% ^{4}He plasmas in ITER.

ASDEX Upgrade (AUG) was the first tokamak that successfully demonstrated this ITER-relevant integrated NBI +ECRF +ICRF scenario for heating H-^{4}He plasmas [10]. Figure 6 shows an example of the application of the three-ion ^{4}He-(^{3}He)-H ICRF scenario with off-axis RF power deposition on AUG (pulse #36751, 2.5T/0.8MA, $f \approx 30$MHz, dipole phasing). In this example, a ramp of ICRF power with off-axis ^{3}He resonance was applied to trigger the L-H transition and associated ELMs, see Fig. 6(b). In fact, different combinations of the heating systems were successfully used to enter the H-mode on AUG, including NBI+ECRF+ICRF (as in ITER), ECRH+ICRF, and ICRF-only. AUG studies also showed that this off-axis ICRF scheme does not lead to tungsten accumulation. The three-ion ^{4}He-(^{3}He)-H ICRF scheme with off-axis ^{3}He resonance was later also successfully applied for heating mixed H + ~10% ^{4}He plasmas (2.5T/2.0MA, $f \approx 33$ MHz) during the past hydrogen campaign at JET.

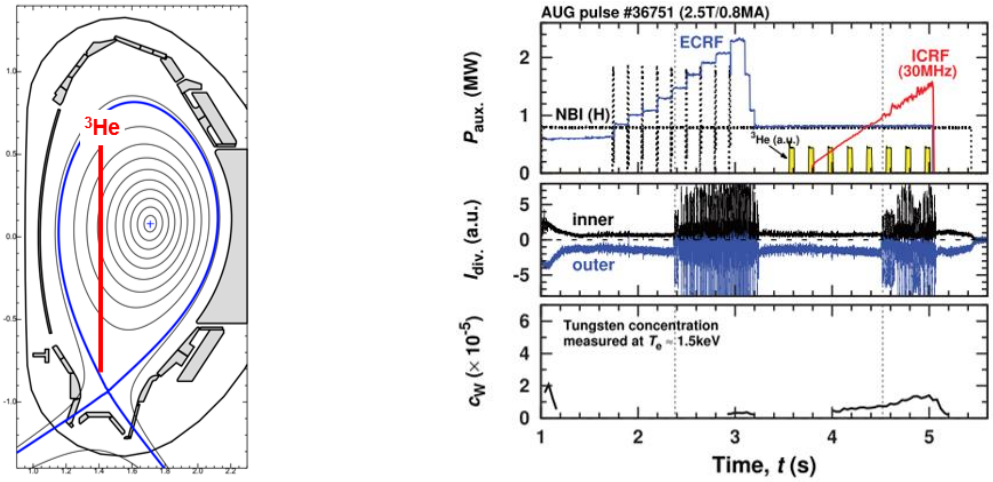

(a) (b)

FIGURE 6. The three-ion ^{4}He-(^{3}He)-H ICRF scenario with off-axis ^{3}He resonance is relevant for heating non-active H + ~10% ^{4}He plasmas in ITER. In combination with the NBI and ECRF heating systems, this integrated heating scenario has the potential to widen the H-mode operational space in ITER. (a) The magnetic configuration of AUG experiments together with the off-axis location of the ^{3}He ion cyclotron resonance in the plasma (2.5T/0.8MA, $f \approx 30$ MHz, dipole phasing). (b) AUG successfully demonstrated the application of this off-axis ICRF heating scenario to trigger ELMs in H-^{4}He plasmas. The vertical dotted lines correspond to L-H transitions and the appearance of ELMs. Figure 6(b) reproduced from Ref. [10].

Because of the limited auxiliary heating power available in this JET campaign (no NBI, $P_{ICRF} \approx 3$-4 MW), JET focused on physics studies with the on-axis ^{4}He-(^{3}He)-H ICRF scheme, see Fig. 7(a). In particular, JET demonstrated the high efficiency of this ICRF scenario for plasma heating using an extremely small amount of ^{3}He ions to absorb RF power, $n(^3\text{He})/n_e \approx 0.2\%$. Efficient plasma heating was shown for a wide range of ^{4}He concentrations, varied between ~5% and ~15%.

In fact, successful results were obtained already in the very first pulse of these studies, see an overview of JET pulse #98423 (3.2T/2.0MA, $n_{e0} \approx 4\times10^{19}$ m^{-3}, $f \approx 33$ MHz, dipole phasing) displayed in Fig. 7(b). The figure shows a clear increase of the plasma stored energy and central electron temperature T_{e0} in response to the stepwise increase of ICRF power. As follows from TRANSP-TORIC modeling, more than 90% of RF power is absorbed by a tiny amount of ^{3}He ions under these conditions, and therefore these ions are accelerated to MeV-range energies. As a result of their collisional slowing down, ICRF-accelerated ^{3}He ions deposit most of their energy to plasma electrons ($E_{crit} \approx 41T_e \approx 160$ keV), thereby leading to core peaked electron heating similar to the conditions expected for alpha heating in ITER and future fusion reactors.

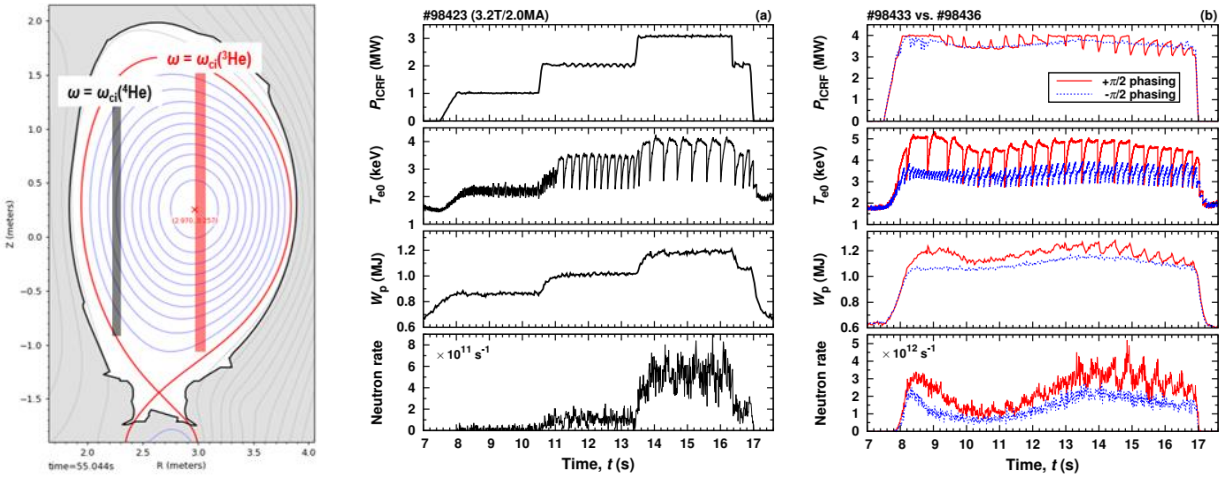

(a) (b) (c)

FIGURE 7. Demonstration of the successful application of the three-ion ^{4}He-(^{3}He)-H ICRF scenario with on-axis ^{3}He resonance in non-active H-^{4}He plasmas at JET. The scheme was efficient for a wide range of ^{4}He concentrations, $n(^4\text{He})/n_e \approx$ 5-15%. (a) The magnetic configuration of JET experiments together with the on-axis location of the ^{3}He ion cyclotron resonance in the plasma (3.2T/2.0MA, $f \approx 33$ MHz). (b) Overview of JET pulse #98423 with $n(^4\text{He})/n_e \approx 13\%$ and $n(^3\text{He})/n_e \approx 0.2\%$ (ICRF: dipole phasing). (c) Overview of JET pulses #98433 ($+\pi/2$ phasing) and #98436 ($-\pi/2$ phasing) with $n(^4\text{He})/n_e \approx 8\%$ and $n(^3\text{He})/n_e \approx 0.2\%$.

The efficient generation of confined energetic ^{3}He ions with ICRF was confirmed by a range of fast-ion diagnostics, including gamma-ray spectroscopy measurements. Furthermore, the presence of fast ^{3}He ions in the plasma led to the destabilization of various AEs and to an increase in the neutron rate, as also seen in Fig. 7(b). In these non-active H-^{4}He plasmas, neutrons originate from the fusion reactions between MeV-range ICRF-accelerated ^{3}He ions and intrinsic ^{9}Be impurities. The assessment of the impact of energetic ions on neutron yield in the pre-DT phase of ITER operations was recently carried out in [40].

The efficiency of fast-ion generation was increased further by reducing the central plasma density to $n_{e0} \approx 3.5\times10^{19}$ m^{-3} and increasing the RF power to ~4MW. This can be seen in Fig. 7(c), showing an overview of JET pulse #98433 (solid lines). In this pulse, an asymmetric $+\pi/2$ ICRF antenna phasing was used. Furthermore, a rich variety of Alfvén eigenmodes was observed in this pulse, including reversed-shear Alfvén eigenmodes (RSAEs). This is an important result which confirms earlier findings that three-ion ICRF scenarios can be efficient in modifying the q-profile in the central regions of JET plasmas [10, 32]. For comparison, we also illustrate the response of the plasma under the same operational conditions, when a different current drive antenna phasing ($-\pi/2$) was applied (pulse #98436). In accordance with theoretical expectations, this resulted in a lower efficiency of fast-ion generation. Figure 7(c) shows a much shorter sawtooth period $\Delta t_{saw} \approx 150$ ms in pulse #98436 (dotted lines), as compared to $\Delta t_{saw} \approx 470$ ms in pulse #98433.

The three-ion ICRF scheme with core ^{3}He heating was also applied on AUG (although in mixed H-D plasmas). As discussed in [10], because of the reduced confinement of MeV-range fast ions in AUG, setting up core plasma heating with this scenario in AUG is more challenging than in a large-scale tokamak JET. Yet a few novel fast-ion measurements were developed with this scenario on AUG, including fast ^{3}He measurements by charge exchange recombination spectroscopy (CXRS) [41] and ^{3}He-driven ion cyclotron emission (ICE) [42].

IMPURITY SEEDING AS A TOOL TO OPTIMIZE ICRF DEPOSITION AND GENERATION OF FAST ^{4}HE IONS

In multi-ion species plasmas, impurity ions can provide a significant contribution to the RF polarization. A combination of intrinsic and extrinsic impurities can be applied as an active tool to control polarization and absorption of RF waves. In this section, we discuss the successful application of impurity seeding on the acceleration of a small amount of ^{4}He ions ($n(^4\text{He})/n_e \approx 0.5\%$) in predominantly hydrogen plasmas at JET-ILW, naturally including a small amount of ^{9}Be impurities ($Z = 4$, $A = 9$, $Z/A \approx 0.44$). Because $(Z/A)_{9\text{Be}} < (Z/A)_{4\text{He}} < (Z/A)_{\text{H}}$, intrinsic ^{9}Be impurities are not resonant absorbers in these plasmas, but are a crucial component that defines the efficiency of acceleration of ^{4}He ions to MeV-range energies with RF waves [43]. The JET experiments reported here complemented earlier studies with the three-ion D-(D_{NBI})-^{3}He scheme for the preparation of alpha particle diagnostics for their future use in the D-T campaign [25].

According to theoretical and modeling results, ^{4}He acceleration to high energies with the three-ion ^{9}Be-(^{4}He)-H ICRF scenario is maximized at ^{9}Be concentrations $n(^9\text{Be})/n_e \approx 1.5\text{-}2.5\%$ [43]. Yet typical concentrations of ^{9}Be impurities in JET-ILW plasmas are lower, $n(^9\text{Be})/n_e \approx 0.5\text{-}1.0\%$. As controlling the concentration of ^{9}Be impurities in the plasma is not straightforward, injecting extrinsic impurities with a similar charge-to-mass ratio (such as $^7\text{Li}^{3+}$, $^{11}\text{B}^{5+}$, $^{22}\text{Ne}^{10+}$, ^{40}Ar, etc.) as an additional control tool was proposed in [10, 43].

Figure 8 shows the first application of this novel technique in JET pulse #98503 (3.47T/2.0MA, $P_{ICRF} \approx 3$MW, $f \approx 29$ MHz, dipole phasing). This pulse was conducted during the past hydrogen campaign at JET, shortly after a series of experiments in H + ~10% ^{4}He plasmas. The residual level of ^{4}He ions in #98503 reached $n(^4\text{He})/n_e \approx 0.5\%$ (no ^{4}He gas was injected in this experiment). Figure 8(a) illustrates the magnetic configuration in this JET pulse, together with the location of the ion cyclotron resonances for different ion species. Under the selected conditions, the cyclotron resonance of resonant ^{4}He ions is located ~30 cm off-axis. Locating the cyclotron resonance of ^{4}He ions in the plasma core requires significantly higher $B_0 \approx 3.85$T. Due to limitations at such high B_0 at JET, plasma operation with this magnetic configuration could not be realized at the time of the experiment.

Figure 8(b) shows an overview of the main parameters in JET pulse #98503, including the plasma stored energy, the central electron temperature, and the neutron rate. Note that these parameters were increased in the last phase of the pulse, when a small amount of ^{22}Ne impurities ($Z = 10$, $A = 22$, $Z/A \approx 0.45$), with a charge-to-mass ratio similar to ^{9}Be impurities, was injected into the plasma. A more efficient sawtooth stabilization was also observed during the phase with ^{22}Ne injection. An efficient generation of MeV-range ^{4}He ions with this novel ^{9}Be/^{22}Ne-(^{4}He)-H ICRF scenario was also confirmed by gamma-ray diagnostics. The isotope ^{22}Ne was deliberately chosen for this proof-of-principle demonstration at JET because of its relatively low ionization energy, $E_{ioniz.} \approx 1.4$ keV. Note that in case of ITER plasmas ($B_0 = 5.3$ T, $f = 40$ MHz, H majority plasmas), the efficiency of this ICRF scenario can be equally tuned with argon impurities ($Z = 18$, $A = 40$, $E_{ioniz.} \approx 4.4$ keV), currently considered for impurity seeding in ITER and future reactors [10].

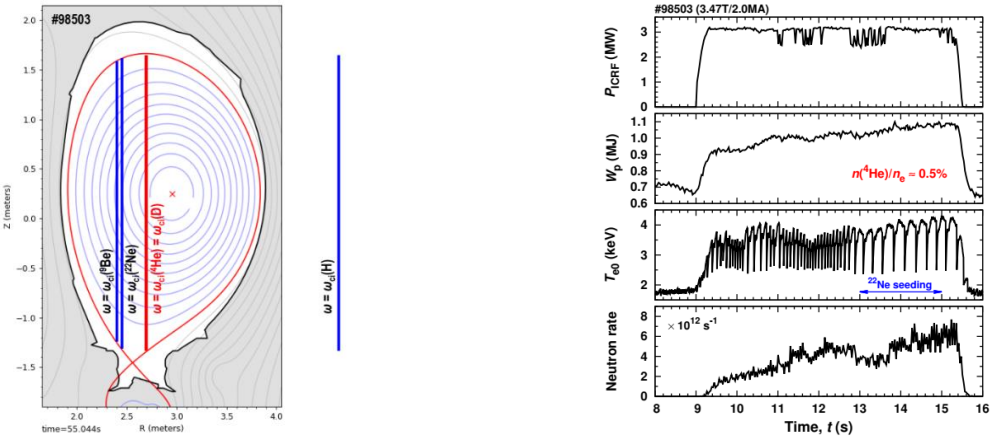

(a) (b)

FIGURE 8. The proof-of-principle demonstration of the three-ion ^{9}Be/^{22}Ne-(^{4}He)-H ICRF scenario for plasma heating and generation of MeV-range ^{4}He ions in H majority plasmas at JET-ILW [10, 43]. (a) The magnetic configuration and the location of ion cyclotron resonances in JET pulse #98503 (3.47T/2.0MA, $f \approx 29$ MHz, dipole phasing). (b) Overview of the main parameters in JET pulse #98503 ($n(^4\text{He})/n_e \approx 0.5\%$). A more efficient generation of high-energy ^{4}He ions was achieved in the last phase of the pulse with an additional injection of ^{22}Ne impurities.

BULK ION HEATING OF D-T ≈ 50%-50% PLASMAS

Several ICRF scenarios relevant for D-T ≈ 50%-50%, tritium and T-rich plasmas were successfully developed and applied for plasma heating during recent tritium and DTE2 campaign at JET-ILW [44-47]. In ITER, second harmonic ICRF heating of the fuel tritium ions, $\omega = 2\omega_{ci}$(T) is considered as the main ICRF heating scenario in D-T ≈ 50%-50% plasmas [2]. This heating scenario also foresees the injection of a few percent of ^{3}He ions to absorb RF power during the ramp-up phase of the pulse, thereby increasing the amount of bulk ion heating. As ^{3}He is a scarce gas, using the three-ion T-(^{9}Be)-D ICRF scenario for increasing T_i in D-T ≈ 50%-50% plasmas and intrinsic ^{9}Be impurities as resonant absorbers was proposed in [48]. Because of their significantly larger critical energy ($E_{crit}(^9\text{Be}) \approx 74T_e$ vs. $E_{crit}(^3\text{He}) \approx 25T_e$), ^{9}Be impurities transfer a larger fraction of absorbed RF power to the fuel D and T ions via Coulomb collisions.

This novel ICRF scenario was successfully demonstrated during the recent DTE2 campaign at JET. Figure 9 shows the application of the T-(^{9}Be)-D ICRF scenario for plasma heating and increasing the ion temperature in JET pulse #99608 (3.7T/2.0MA, L-mode, D-T ≈ 50%-50%, $f \approx 25$MHz, dipole phasing). Under these conditions, the ion cyclotron resonance of ^{9}Be impurities is located in the plasma core. In accordance with theoretical predictions, a strong increase in T_i was observed when about 2 MW of ICRF power was coupled to this plasma. The core-localized generation of fusion-born alpha particles was confirmed by neutron and gamma-ray diagnostics. The three-ion ICRF scheme was also successfully tested for heating H-mode D-T plasmas during the last day of the DTE2 campaign. In particular, about 8 MW fusion power was sustained for 2.5 s with the combination of high-power NBI heating (~29 MW) and ~1.7 MW of the three-ion ICRF scheme.

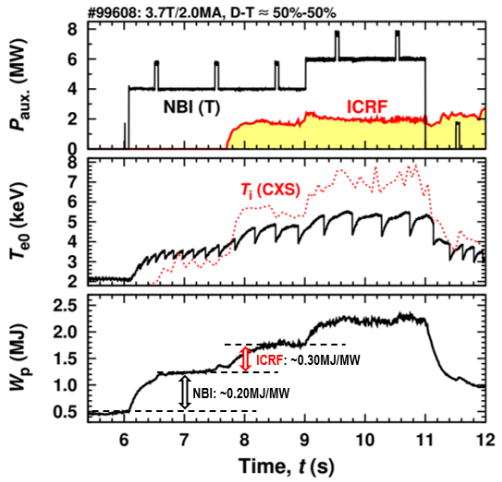

FIGURE 9. The ITER-relevant three-ion T-(^{9}Be)-D ICRF scenario using intrinsic ^{9}Be impurities as resonant absorbers was successfully demonstrated for plasma heating and increasing T_i in D-T ≈ 50%-50% plasmas at JET-ILW (pulse #99608, 3.7T/2.0MA, $f \approx 25$ MHz, dipole phasing).

As discussed in [10, 48], the three-ion T-(^{9}Be)-D ICRF scenario is also compatible with additional seeding of ^{7}Li, ^{11}B, ^{22}Ne and Ar impurities, extending the possible application of this scenario in ITER and future fusion reactors. The experimental study of the combined Ar and ^{9}Be ICRF heating of D-T plasmas was planned as a part of DTE2 studies, but was not demonstrated because of the limited machine time.

Note that off-axis plasma heating with the similar T-(^{7}Li)-D ICRF scenario was already observed in the past D-T experiments on TFTR, but was considered as a parasitic ^{7}Li impurity absorption [49]. Recently, the application of this ICRF scenario was revisited and the three-ion T-(^{7}Li)-D ICRF scenario was proposed for bulk ion heating in CFETR [50].

SUMMARY AND CONCLUSIONS

Recent progress with the development of the three-ion ICRF scenarios on the tokamaks Alcator C-Mod, ASDEX Upgrade and JET have converted these scenarios into a versatile tool for plasma heating and fast-ion studies [8, 10]. Tuned for the central deposition of RF power and maximizing the fast-ion pressure in the plasma core, these scenarios allow to get a better understanding of plasmas with core electron heating from MeV-range fast ions. The analysis of dedicated JET experiments in D-^{3}He plasmas revealed a range of new fast-ion physics phenomena, relevant for ITER and future fusion reactors with dominant alpha particle heating. In particular, improved thermal ion confinement was observed in JET plasmas with a large amount of MeV-range fast ions in the presence of TAE modes [27]. JET experiments also revealed the potential of three-ion ICRF scenarios to generate a large population of passing fast ions (similar to fast ions from N-NBI) [10]. In turn, these fast ions are efficient in local current drive, resulting in an inverted q-profile and leading to a novel observation of high-frequency reversed-shear AEs at JET [32].

Three-ion ICRF scenarios are also relevant for plasma operations in ITER. Significant progress with the development of these novel scenarios in view of their applications in non-active and D-T plasmas of ITER was recently achieved on JET and AUG. In particular, AUG prototyped the combined NBI, ECRF and ICRF heating scenario in non-active H-^{4}He plasmas having the potential to widen the H-mode operational space in ITER [10]. The on-axis and off-axis plasma heating with the three-ion ^{4}He-(^{3}He)-H ICRF scenario was also later demonstrated at JET. Finally, recent JET experiments in non-active and D-T plasmas illustrated that these novel ICRF scenarios can profit from the presence of low-*Z* and mid-*Z* impurities in the plasma. In particular, JET confirmed the beneficial impact of seeding Be-like impurities (e.g., ^{22}Ne) on the generation of MeV-range ^{4}He ions in predominantly hydrogen plasma. Furthermore, dedicated ICRF experiments with the ITER-relevant three-ion T-(^{9}Be)-D scenario during DTE2 campaign at JET confirmed the potential of this novel scenario for bulk ion heating and increasing the ion temperature in L-mode D-T ≈ 50%-50% plasmas.

ACKNOWLEDGMENTS

This work has been carried out within the framework of the EUROfusion Consortium, funded by the European Union via the Euratom Research and Training Programme (Grant Agreement No 101052200 – EUROfusion). Views and opinions expressed are however those of the author(s) only and do not necessarily reflect those of the European Union or the European Commission. Neither the European Union nor the European Commission can be held responsible for them. We thank the ITPA Energetic Particle Physics Topical Group for its support. Part of this work was also carried out in the framework of projects done for the ITER Scientist Fellow Network (ISFN).

ITER is the Nuclear Facility INB No. 174. The views and opinions expressed herein do not necessarily reflect those of the ITER Organization. This publication is provided for scientific purposes only. Its contents should not be considered as commitments from the ITER Organization as a nuclear operator in the frame of the licensing process.

REFERENCES

1. M. Porkolab et al., AIP Conf. Proc. **314**, 99 (1994)
2. ITER Physics Basis Expert Group on Energetic Particles, Heating and Current Drive and ITER Physics Basis Editors, Nucl. Fusion **39**, 2495 (1999)
3. J. Ongena et al., Plasma Phys. Control. Fusion **59**, 054002 (2017)
4. J.R. Wilson and P.T. Bonoli, Phys. Plasmas **22**, 021801 (2015)
5. T.H. Stix, Nucl. Fusion **15**, 737 (1975)
6. T.H. Stix, Plasma Phys. **14**, 367 (1972)
7. Ye.O. Kazakov et al., Nucl. Fusion **55**, 032001 (2015)
8. Ye.O. Kazakov et al., Nature Physics **13**, 973 (2017)
9. J. Ongena et al., EPJ Web Conf. **157**, 02006 (2017)
10. Ye.O. Kazakov et al., Phys. Plasmas **28**, 020501 (2021)
11. Y. Lin et al., EPJ Web Conf. **157**, 03030 (2017)
12. D. Van Eester et al., Plasma Phys. Control. Fusion **59**, 085012 (2017)
13. Ye.O. Kazakov et al., AIP Conf. Proc. **1689**, 030008 (2015)
14. L.-G. Eriksson et al., Phys. Rev. Lett. **81**, 1231 (1998)
15. M.J. Mantsinen et al., Phys. Rev. Lett. **89**, 115004 (2002)
16. H. Järleblad et al., Nucl. Fusion **62**, 112005 (2022)
17. Ye.O. Kazakov et al., Nucl. Fusion **60**, 112013 (2020)
18. K. Kirov et al., AIP Conf. Proc. **2254**, 030011 (2020)
19. M.J. Mantsinen et al., Proc. 46th EPS Conf. on Plasma Physics, O5.102 (2019)
20. A. Sahlberg et al., Nucl. Fusion **61**, 036025 (2021)
21. V. Bobkov et al., AIP Conf. Proc. **2254**, 040005 (2020)
22. J. Garcia et al., Phys. Plasmas **25**, 055902 (2018)
23. S. Pinches et al., Phys. Plasmas **22**, 021807 (2015)
24. M. Nocente et al., Nucl. Fusion **60**, 124006 (2020)
25. E. Panotin et al., Rev. Sci. Instrum. **92**, 053529 (2021)

26. J. Mailloux et al., Nucl. Fusion **62**, 042026 (2022)
27. S. Mazzi et al., Nature Physics **18**, 776 (2022)
28. S. Mazzi et al., Plasma Phys. Control. Fusion **64**, 114001 (2022)
29. Ž. Štancar et al., Nucl. Fusion **61**, 126030 (2021)
30. A. Tinguely et al., Nucl. Fusion **62**, 076001 (2022)
31. A. Tinguely et al., Nucl. Fusion **62**, 112008 (2022)
32. M. Dreval et al., Nucl. Fusion **62**, 056001 (2022)
33. V.G. Kiptily et al., Nucl. Fusion **61**, 114006 (2021)
34. V.G. Kiptily et al., Plasma Phys. Control. Fusion **64**, 064001 (2022)
35. M. Takechi et al., Phys. Plasmas **12**, 082509 (2005)
36. A. Bierwage et al., Nature Comm. **13**, 3941 (2022)
37. B. Bigot, Nucl. Fusion **59**, 112001 (2019)
38. J.C. Hillesheim et al., Proc. 44th EPS Conf. on Plasma Physics, P5.162 (2017)
39. M. Schneider et al., EPJ Web Conf. **157**, 03046 (2017)
40. A. Polevoi et al., Nucl. Fusion **61**, 076008 (2021)
41. A. Kappatou et al., Nucl. Fusion **61**, 036017 (2021)
42. R. Ochoukov et al., AIP Conf. Proc. **2254**, 030005 (2020)
43. Ye.O. Kazakov et al., Proc. 45th EPS Conf. on Plasma Physics, P5.1047 (2018)
44. P. Jacquet et al., "ICRH operations and experiments during the JET-ILW tritium and DTE2 campaign", this conference
45. K. Kirov et al., "Impact of ICRH heating of fast D and T ions on fusion performance in JET DTE2 campaign", this conference
46. E. Lerche et al., "Fundamental ICRF heating of Deuterium ions in JET-DTE2", this conference
47. D. Van Eester et al., "RF power as key contributor to high performance baseline scenario experiments in JET DD and DT plasmas in preparation for ITER", this conference
48. Ye.O. Kazakov et al., Phys. Plasmas **22**, 082511 (2015)
49. J.R. Wilson et al., Phys. Plasmas **5**, 1721 (1998)
50. C. Song et al., Physica Scripta **96**, 025603 (2021)